RESEARCH REPORT SERIES no. 53-2012

FOREST OF DEAN ARCHAEOLOGICAL SURVEY
SCIENTIFIC DATING OF EARTHWORK SYSTEMS SO6013/04 AND SO6013/26

SCIENTIFIC DATING REPORT

Phillip Toms, Gordon Cook, Christopher Bronk Ramsey and Alex Bayliss

INTERVENTION
AND ANALYSIS

ENGLISH HERITAGE

This report has been prepared for use on the internet and the images within it have been down-sampled to optimise downloading and printing speeds.

Please note that as a result of this down-sampling the images are not of the highest quality and some of the fine detail may be lost. Any person wishing to obtain a high resolution copy of this report should refer to the ordering information on the following page.

Research Report Series 53-2012

FOREST OF DEAN ARCHAEOLOGICAL SURVEY

SCIENTIFIC DATING OF EARTHWORK SYSTEMS SO6013/04 AND SO6013/26

Phillip Toms, Gordon Cook, Christopher Bronk Ramsey, and Alex Bayliss

NGR: 306950 213030

ISSN 2046-9799 (Print)
ISSN 2046-9802 (Online)

The Research Report Series incorporates reports by the expert teams within the Investigation & Analysis Division of the Heritage Protection Department of English Heritage, alongside contributions from other parts of the organisation. It replaces the former Centre for Archaeology Reports Series, the Archaeological Investigation Report Series, the Architectural Investigation Report Series, and the Research Department Report Series.

Many of the Research Reports are of an interim nature and serve to make available the results of specialist investigations in advance of full publication. They are not usually subject to external refereeing, and their conclusions may sometimes have to be modified in the light of information not available at the time of the investigation. Where no final project report is available, readers must consult the author before citing these reports in any publication. Opinions expressed in Research Reports are those of the author(s) and are not necessarily those of English Heritage.

Requests for further hard copies, after the initial print run, can be made by emailing:
Res.reports@english-heritage.org.uk
or by writing to:
English Heritage, Fort Cumberland, Fort Cumberland Road, Eastney, Portsmouth PO4 9LD
Please note that a charge will be made to cover printing and postage.

SUMMARY

A series of radiocarbon dates and optically stimulated luminescence ages were obtained from colluvium and overlying deposits, which had built up behind a bank related to earthwork system so6013/04. Bayesian chronological modelling of these scientific dates, along with the recorded stratigraphic sequence, suggests that this earthwork system may have been laid out in the mid first millennium cal BC. An overlying deposit containing iron-working debris, probably dates to the late first or early second century cal AD. Two ages were obtained by optically stimulated luminescence from colluvium that may be related to earthwork system so6013/26. These dates demonstrate that this earthwork system was laid out in, or after, the latter part of the first millennium cal BC.

CONTRIBUTORS

Phillip Toms, Luminescence dating laboratory, School of Natural and Social Sciences, University of Gloucestershire, Swindon Road, Cheltenham GL50 4AZ

Gordon Cook, Scottish Universities Environmental Research Centre, Scottish Enterprise Technology Park, Rankine Avenue, East Kilbride G75 0QF

Christopher Bronk Ramsey, Oxford Radiocarbon Accelerator Unit, Dyson Perrins Building, South Parks Road, Oxford OX1 3QY

Alex Bayliss, English Heritage, 1 Waterhouse Square, 138–142 Holborn, London EC1N 2ST

ACKNOWLEDGEMENTS

We thank Jon Hoyle of Gloucestershire County Council for helpful comments on this report and for the provision of Figures 1 and 2, Shahina Farid of English Heritage for help with the production of this report, and English Heritage for funding this research.

ARCHIVE LOCATION

Gloucestershire Historic Environment Record, Gloucestershire County Council, Shire Hall, Westgate Street, Gloucester GL1 2TG

DATE OF RESEARCH

2011

CONTACT DETAILS

Phillip Toms, Luminescence dating laboratory, School of Natural and Social Sciences, University of Gloucestershire, Swindon Road, Cheltenham GL50 4AZ
ptoms@glos.ac.uk; 01242 714708

Gordon Cook, Scottish Universities Environmental Research Centre, Scottish Enterprise Technology Park, Rankine Avenue, East Kilbride G75 0QF
Gordon.Cook@glasgow.ac.uk 01355 270136

Christopher Bronk Ramsey, Oxford Radiocarbon Accelerator Unit, Dyson Perrins Building, South Parks Road, Oxford OX1 3QY
Christopher.ramsey@rlaha.ox.ac.uk 01865 285229

Alex Bayliss, English Heritage, 1 Waterhouse Square, 138–142 Holborn, London EC1N 2ST
alex.bayliss@english-heritage.org.uk 0207 9733299

CONTENTS

1. INTRODUCTION

The Forest of Dean Archaeological Survey comprises a phased programme of desk-based data collection, pilot field survey, lidar survey and analysis, and rapid survey of selected earthworks detected by lidar.

Earthwork systems so6013/04 (NGR 360809 213209) and so6013/26 (NGR 360433 212957) are situated in West Dean parish on the western side of the Lyd/Cannop Brook valley. Earthwork system so6013/04 is situated on an east facing slope rising from *c* 100m AOD to *c* 135m AOD, and consists of a rectilinear pattern of terraces which both follow and cross the natural contours of the valley side. Earthwork system so6013/26, to its west, is situated on an east–southeast facing slope at heights of between *c* 120 and 145m AOD. The earthworks in this system consist of a series of parallel linear terraces which run from east to west up the predominant natural slope, but across the gentler slope.

Trench 1 was cut across the southeastern part of earthwork system so6013/04. This revealed a series of layers containing abundant charcoal fragments, bloomery slag, and burnt ceramic material identified as bloomery furnace lining material (contexts (105)/(101)/(114)/(115)/(116)). Below this lay a thick deposit of colluvium (103/107/109), which appeared to be revetted by a low bank (104), suggesting the laying out of a boundary system followed by a period in which soil up slope was loosened and accumulated against the back of the bank.

Trench 2 was cut across the southern part of earthwork system so6013/26. It revealed colluvium (context (201)) over natural deposits.

2. SAMPLING

Two fragments of roundwood charcoal were sampled for radiocarbon dating from context (116) in Trench 1, and a sample of sediment was taken for optically stimulated luminescence dating from the underlying, colluvial context (103). The earlier layer of colluvium, (107), was sampled for both optically stimulated luminescence dating and radiocarbon dating (Fig 1).

In Trench 2, samples from the lower and upper parts of context (201) were taken for optically stimulated luminescence dating (Fig 2).

3. RADIOCARBON DATING

Two samples of short-lived charcoal were dated from Trench 1, contexts (116) and (107). One sample from each context was dated at the Scottish Universities Environmental Research Centre (SUERC), and the other was dated at the Oxford Radiocarbon Accelerator Unit (OxA).

Samples dated at SUERC were prepared using methods outlined in Stenhouse and Baxter (1983), combusted to carbon dioxide (Vandeputte *et al* 1996), graphitized (Slota *et al* 1987), and measured by accelerator mass spectrometry (AMS) as described by Xu *et al* (2004). The samples dated at ORAU were processed using methods outlined in Brock *et al* (2010), graphitized (Dee and Bronk Ramsey 2000), and measured by AMS as described by Bronk Ramsey *et al* (2004).

Both laboratories maintain continual programmes of quality assurance, in addition to participation in international inter-comparisons (Scott *et al* 2010). These tests indicate no laboratory offsets and demonstrate the validity of the precision quoted.

The results are conventional radiocarbon ages (Stuiver and Polach 1977), and are quoted in accordance with the international standard known as the Trondheim convention (Stuiver and Kra 1986). The calibrated date ranges in Table 1 have been calculated using the maximum intercept method (Stuiver and Reimer 1986), the calibration curve of Reimer *et al* (2009; IntCal09), and the computer program OxCal v4.1 (Bronk Ramsey 1995; 1998; 2001; 2009). They are rounded outwards to10 years.

The two measurements from context (116) are statistically consistent (T'=2.6; T'(5%)=3.8; ν=1; Ward and Wilson 1978), as are the two measurements from context (107) (T'=2.4; T'(5%)=3.8; ν=1). This suggests that the dated material may relate to a coherent episode of activity, probably the iron smelting represented by the bloomery waste in the case of context (116), rather than being residual material incorporated into these contexts by chance.

4. OPTICALLY STIMULATED LUMINESCENCE DATING

4.1 Mechanisms and principles

Upon exposure to ionising radiation, electrons within the crystal lattice of insulating minerals are displaced from their atomic orbits. Whilst this dislocation is momentary for most electrons, a portion of charge is redistributed to meta-stable sites (traps) within the crystal lattice. In the absence of significant optical and thermal stimuli, this charge can be stored for extensive periods. The quantity of charge relocation and storage relates to the magnitude and period of irradiation. When the lattice is optically or thermally stimulated, charge is evicted from traps and may return to a vacant orbit position (hole). Upon recombination with a hole, an electron's energy can be dissipated in the form of light generating crystal luminescence providing a measure of dose absorption.

Herein, quartz is segregated for dating. The utility of this minerogenic dosimeter lies in the stability of its datable signal over the mid to late Quaternary period, predicted through isothermal decay studies (eg Smith *et al* 1990; retention lifetime 630Ma at 20°C) and evidenced by optical age estimates concordant with independent chronological controls (eg Murray and Olley 2002). This stability is in contrast to the anomalous fading of

comparable signals commonly observed for other ubiquitous sedimentary minerals such as feldspar and zircon (Wintle 1973; Templer 1985; Spooner 1993).

Optical age estimates of sedimentation (Huntley *et al* 1985) are premised upon reduction of the minerogenic time dependent signal (Optically Stimulated Luminescence, OSL) to zero through exposure to sunlight and, once buried, signal reformulation by absorption of litho- and cosmogenic radiation. The signal accumulated post-burial acts as a dosimeter recording total dose absorption, converting to a chronometer by estimating the rate of dose absorption quantified through the assay of radioactivity in the surrounding lithology and streaming from the cosmos.

$$\text{Age} = \frac{\text{Mean Equivalent Dose } (D_e, \text{ Gy})}{\text{Mean Dose Rate } (D_r, \text{ Gy.ka}^{-1})}$$

Aitken (1998) and Bøtter-Jensen *et al* (2003) offer a detailed review of optical dating.

4.2 Sample Collection and Preparation

A total of four sediment samples were collected within opaque plastic tubing from section faces in two trenches of the Forest of Dean Archaeological Survey (Table 2a–b; Figs 1–2). Each tube was wrapped in cellophane and parcel tape, and then marked indelibly with a field code. Each sample hole was excavated further for *in situ* NaI gamma spectrometry. An additional 100g of sediment from within each sample hole was collected for *ex situ* Ge gamma spectrometry.

To preclude optical erosion of the datable signal prior to measurement, all samples were prepared under controlled laboratory illumination provided by Encapsulite RB-10 (red) filters. To isolate that material potentially exposed to daylight during sampling, sediment located within 20mm of each tube-end was removed.

The remaining sample was dried and then sieved. Quartz within the fine sand (125-180μm or 180-250μm) fraction was segregated. Samples were then subjected to acid and alkaline digestion (10% HCl, 15% H_2O_2) to attain removal of carbonate and organic components respectively. A further acid digestion in HF (40%, 60mins) was used to etch the outer 10-15μm layer affected by α radiation and degrade each samples' feldspar content. During HF treatment, continuous magnetic stirring was used to effect isotropic etching of grains. 10% HCl was then added to remove acid soluble fluorides. Each sample was dried, resieved, and quartz isolated from the remaining heavy mineral fraction using a sodium polytungstate density separation at 2.68g.cm^{-3}. Twelve multi-grain aliquots (*c* 3-6mg) of quartz from each sample (5 aliquots in the case of sample GL11020) were then mounted on aluminium discs for determination of D_e values.

All drying was conducted at 40°C to prevent thermal erosion of the signal. All acids and alkalis were Analar grade. All dilutions (removing toxic-corrosive and non-minerogenic luminescence-bearing substances) were conducted with distilled water to prevent signal contamination by extraneous particles.

4.3 Acquisition and accuracy of D_e value

All minerals naturally exhibit marked inter-sample variability in luminescence per unit dose (sensitivity). Therefore, the estimation of D_e acquired since burial requires calibration of the natural signal using known amounts of laboratory dose. D_e values were quantified using a single-aliquot regenerative-dose (SAR) protocol (Murray and Wintle 2000; 2003) facilitated by a Risø TL-DA-15 irradiation-stimulation-detection system (Markey *et al* 1997; Bøtter-Jensen *et al* 1999). Within this apparatus, optical signal stimulation is provided by an assembly of blue diodes (5 packs of 6 Nichia NSPB500S), filtered to 470±80nm conveying 15mW.cm^{-2} using a 3mm Schott GG420 positioned in front of each diode pack. Infrared (IR) stimulation, provided by 6 IR diodes (Telefunken TSHA 6203) stimulating at 875±80nm delivering ~5 mW.cm^{-2}, was used to indicate the presence of contaminant feldspars (Hütt *et al* 1988). Stimulated photon emissions from quartz aliquots are in the ultraviolet (UV) range and were filtered from stimulating photons by 7.5mm HOYA U-340 glass and detected by an EMI 9235QA photomultiplier fitted with a blue-green sensitive bialkali photocathode. Aliquot irradiation was conducted using a 1.48 GBq ^{90}Sr/^{90}Y β source calibrated for multi-grain aliquots fine quartz sand against the 'Hotspot 800' ^{60}Co γ source located at the National Physical Laboratory (NPL), UK.

SAR by definition evaluates D_e through measuring the natural signal (Fig 3) of a single aliquot and then regenerating that aliquot's signal by using known laboratory doses to enable calibration. For each aliquot, five different regenerative-doses were administered so as to image dose response. D_e values for each aliquot were then interpolated, and associated counting and fitting errors calculated, by way of exponential regression (Fig 3). Weighted (geometric) mean D_e values were calculated, given sufficient mass, from 12 aliquots using the central age model outlined by Galbraith *et al* (1999) and are quoted at 1σ confidence. The accuracy with which D_e equates to total absorbed dose and that dose absorbed since burial was assessed. The former can be considered a function of laboratory factors, the latter, one of environmental issues. Diagnostics were deployed to estimate the influence of these factors and criteria instituted to optimise the accuracy of D_e values.

4.3.1 Laboratory Factors

Feldspar contamination

The propensity of feldspar signals to fade and underestimate age, coupled with their higher sensitivity relative to quartz makes it imperative to quantify feldspar contamination.

At room temperature, feldspars generate a signal (IRSL) upon exposure to IR whereas quartz does not. The signal from feldspars contributing to OSL can be depleted by prior exposure to IR. For all aliquots the contribution of any remaining feldspars was estimated from the OSL IR depletion ratio (Duller 2003). If the addition to OSL by feldspars is insignificant, then the repeat dose ratio of OSL to post-IR OSL should be statistically consistent with unity (Figs 3 and 7). If any aliquots do not fulfil this criterion, then the sample age estimate should be accepted tentatively. The source of feldspar contamination is rarely rooted in sample preparation; it predominantly results from the occurrence of feldspars as inclusions within quartz.

Preheating

Preheating aliquots between irradiation and optical stimulation is necessary to ensure comparability between natural and laboratory-induced signals. However, the multiple irradiation and preheating steps that are required to define single-aliquot regenerative-dose response leads to signal sensitisation, rendering calibration of the natural signal inaccurate. The SAR protocol (Murray and Wintle 2000; 2003) enables this sensitisation to be monitored and corrected using a test dose, here set at 5Gy preheated to 220°C for 10s, to track signal sensitivity between irradiation-preheat steps. However, the accuracy of sensitisation correction for both natural and laboratory signals can be preheat dependent.

The Dose Recovery test was used to assess the optimal preheat temperature for accurate correction and calibration of the time dependent signal. Dose Recovery (Fig 4) attempts to quantify the combined effects of thermal transfer and sensitisation on the natural signal, using a precise lab dose to simulate natural dose. The ratio between the applied dose and recovered D_e value should be statistically concordant with unity. For this diagnostic, six aliquots were each assigned a 10s preheat between 180°C and 280°C.

That preheat treatment fulfilling the criterion of accuracy within the Dose Recovery test was selected to generate the final D_e value from a further 12 aliquots. Further thermal treatments, prescribed by Murray and Wintle (2000; 2003), were applied to optimise accuracy and precision. Optical stimulation occurred at 125ºC in order to minimise effects associated with photo-transferred thermoluminescence and maximise signal to noise ratios. Inter-cycle optical stimulation was conducted at 280ºC to minimise recuperation.

Irradiation

For all samples having D_e values in excess of 100Gy, matters of signal saturation and laboratory irradiation effects are of concern. With regards the former, the rate of signal accumulation generally adheres to a saturating exponential form and it is this that limits the precision and accuracy of D_e values for samples having absorbed large doses. For such samples, the functional range of D_e interpolation by SAR has been verified up to 600Gy

by Pawley *et al* (2010). Age estimates based on D_e values exceeding this value should be accepted tentatively.

Internal consistency

Quasi-radial plots (cf Galbraith 1990) are used to illustrate inter-aliquot D_e variability for natural, repeat regenerative-dose and OSL to post-IR OSL signals (Figs 5–7 respectively). D_e values are standardised relative to the central D_e value for natural signals and applied dose for regenerated signals. D_e values are described as overdispersed when >5% lie beyond $\pm 2\sigma$ of the standardising value; resulting from a heterogeneous absorption of burial dose and/or response to the SAR protocol. For multi-grain aliquots, overdispersion of natural signals does not necessarily imply inaccuracy. However where overdispersion is observed for regenerated signals, the efficacy of sensitivity correction may be problematic. This measure of SAR protocol success at Gloucestershire differs and is more stringent than that prescribed by Murray and Wintle (2000; 2003). They suggest repeat dose ratios (Table 2b) should be concordant with the range 0.9-1.1; this filter of analytical validity has been applied in this study.

4.3.2 Environmental factors

Incomplete zeroing

Post-burial OSL signals residual of pre-burial dose absorption can result where pre-burial sunlight exposure is limited in spectrum, intensity, and/or period, leading to age overestimation. This effect is particularly acute for material eroded and redeposited sub-aqueously (Olley *et al* 1998, 1999; Wallinga 2002) and exposed to a burial dose of <20 Gy (eg Olley *et al* 2004), has some influence in sub-aerial contexts but is rarely of consequence where aerial transport has occurred. Within single-aliquot regenerative-dose optical dating there are two diagnostics of partial resetting (or bleaching); signal analysis (Agersnap-Larsen *et al* 2000; Bailey *et al* 2003) and inter-aliquot D_e distribution studies (Murray *et al* 1995).

Within this study, signal analysis was used to quantify the change in D_e value with respect to optical stimulation time for multi-grain aliquots. This exploits the existence of traps within minerogenic dosimeters that bleach with different efficiency for a given wavelength of light to verify partial bleaching. D_e (t) plots (Fig 8; Bailey *et al* 2003) are constructed from separate integrals of signal decay as laboratory optical stimulation progresses. A statistically significant increase in natural D_e (t) is indicative of partial bleaching assuming three conditions are fulfilled. Firstly, that a statistically significant increase in D_e (t) is observed when partial bleaching is simulated within the laboratory. Secondly, that there is no significant rise in D_e (t) when full bleaching is simulated. Finally, there should be no significant augmentation in D_e (t) when zero dose is simulated. Where partial bleaching is detected, the age derived from the sample should be considered a maximum estimate

only. However, the utility of signal analysis is strongly dependent upon a samples pre-burial experience of sunlight's spectrum and its residual to post-burial signal ratio. Given in the majority of cases, the spectral exposure history of a deposit is uncertain, the absence of an increase in natural D_e (t) does not necessarily testify to the absence of partial bleaching.

Where requested and feasible, the insensitivities of multi-grain single-aliquot signal analysis may be circumvented by inter-aliquot D_e distribution studies. This analysis uses aliquots of single sand grains to quantify inter-grain D_e distribution. At present, it is contended that asymmetric inter-grain D_e distributions are symptomatic of partial bleaching and/or pedoturbation (Murray *et al* 1995; Olley *et al* 1999; Olley *et al* 2004; Bateman *et al* 2003). For partial bleaching at least, it is further contended that the D_e acquired during burial is located in the minimum region of such ranges. The mean and breadth of this minimum region is the subject of current debate, as it is additionally influenced by heterogeneity in microdosimetry, variable inter-grain response to SAR, and residual to post-burial signal ratios. Presently, the apposite measure of age is that defined by the D_e interval delimited by the minimum and central age models of Galbraith *et al* (1999).

Pedoturbation

The accuracy of sedimentation ages can further be controlled by post-burial trans-strata grain movements forced by pedo- or cryoturbation. Berger (2003) contends pedogenesis prompts a reduction in the apparent sedimentation age of parent material through bioturbation and illuviation of younger material from above and/or by biological recycling and resetting of the datable signal of surface material. Berger (2003) proposes that the chronological products of this remobilisation are A-horizon age estimates reflecting the cessation of pedogenic activity, Bc/C-horizon ages delimiting the maximum age for the initiation of pedogenesis with estimates obtained from Bt-horizons providing an intermediate age 'close to the age of cessation of soil development'. Singhvi *et al* (2001), in contrast, suggest that B and C-horizons closely approximate the age of the parent material, the A-horizon, that of the 'soil forming episode'. At present there is no post-sampling mechanism for the direct detection of and correction for post-burial sediment remobilisation. However, intervals of palaeosol evolution can be delimited by a maximum age derived from parent material and a minimum age obtained from a unit overlying the palaeosol. Inaccuracy forced by cryoturbation may be bidirectional, heaving older material upwards or drawing younger material downwards into the level to be dated. Cryogenic deformation of matrix-supported material is, typically, visible; sampling of such cryogenically-disturbed sediments can be avoided.

4.4 Acquisition and accuracy of D_r value

Lithogenic D_r values were defined through measurement of U, Th, and K radionuclide concentration and conversion of these quantities into β and γ D_r values (Table 2a). β

contributions were estimated from sub-samples by laboratory-based γ spectrometry using an Ortec GEM-S high purity Ge coaxial detector system, calibrated using certified reference materials supplied by CANMET. γ dose rates were estimated from *in situ* NaI gamma spectrometry. These measurements were conducted using an EG&G μNomad portable NaI gamma spectrometer (calibrated using the block standards at RLAHA, University of Oxford) and reduce uncertainty relating to potential heterogeneity in the γ field surrounding each sample. The level of U disequilibrium was estimated by laboratory-based Ge γ spectrometry. Estimates of radionuclide concentration were converted into D_r values (Adamiec and Aitken 1998), accounting for D_r modulation forced by grain size (Mejdahl 1979) and present moisture content (Zimmerman 1971). Cosmogenic D_r values were calculated on the basis of sample depth, geographical position, and matrix density (Prescott and Hutton 1994).

The spatio-temporal validity of D_r values can be considered a function of five variables. Firstly, age estimates devoid of *in situ* γ spectrometry data should be accepted tentatively if the sampled unit is heterogeneous in texture or if the sample is located within 300mm of strata consisting of differing texture and/or mineralogy. However, where samples are obtained throughout a vertical profile, consistent values of γ D_r based solely on laboratory measurements may evidence the homogeneity of the γ field and hence accuracy of γ D_r values. Secondly, disequilibrium can force temporal instability in U and Th emissions. The impact of this infrequent phenomenon (Olley *et al* 1996) upon age estimates is usually insignificant given their associated margins of error. However, for samples where this effect is pronounced (>50% disequilibrium between ^{238}U and ^{226}Ra; Fig 9), the resulting age estimates should be accepted tentatively. Thirdly, pedogenically-induced variations in matrix composition of B and C-horizons, such as radionuclide and/or mineral remobilisation, may alter the rate of energy emission and/or absorption. If D_r is invariant through a dated profile and samples encompass primary parent material, then element mobility is likely limited in effect. Fourthly, spatio-temporal detractions from present moisture content are difficult to assess directly, requiring knowledge of the magnitude and timing of differing contents. However, the maximum influence of moisture content variations can be delimited by recalculating D_r for minimum (zero) and maximum (saturation) content. Finally, temporal alteration in the thickness of overburden alters cosmic D_r values. Cosmic D_r often forms a negligible portion of total D_r. It is possible to quantify the maximum influence of overburden flux by recalculating D_r for minimum (zero) and maximum (surface sample) cosmic D_r.

4.5 Estimation of Age

Age estimates reported in Table 2b provide an estimate of sediment burial period based on mean D_e and D_r values and their associated analytical uncertainties. Uncertainty in age estimates is reported as a product of systematic and experimental errors, with the magnitude of experimental errors alone shown in parenthesis (Table 2b). Probability distributions indicate the inter-aliquot variability in age (Fig 10). The maximum influence of

temporal variations in D_r forced by minima-maxima in moisture content and overburden thickness is illustrated in Figure 10. Where uncertainty in these parameters exists this age range may prove instructive, however the combined extremes represented should not be construed as preferred age estimates. The analytical validity of each sample is presented in Table 3.

4.6 Analytical uncertainty

All errors are based upon analytical uncertainty and quoted at 1σ confidence. Error calculations account for the propagation of systematic and/or experimental (random) errors associated with D_e and D_r values.

For D_e values, systematic errors are confined to laboratory β source calibration. Uncertainty in this respect is that combined from the delivery of the calibrating γ dose (1.2%; NPL pers comm), the conversion of this dose for SiO_2 using the respective mass energy-absorption coefficient (2%; Hubbell 1982) and experimental error, totalling 3.5%. Mass attenuation and bremsstrahlung losses during γ dose delivery are considered negligible. Experimental errors relate to D_e interpolation using sensitisation corrected dose responses. Natural and regenerated sensitisation corrected dose points (S_i) were quantified by,

$$S_i = (D_i - x.L_i) / (d_i - x.L_i) \qquad \textbf{Eq.1}$$

where D_i = Natural or regenerated OSL, initial 0.2s
L_i = Background natural or regenerated OSL, final 5s
d_i = Test dose OSL, initial 0.2s
x = Scaling factor, 0.08

The error on each signal parameter is based on counting statistics, reflected by the square-root of measured values. The propagation of these errors within Eq. 1 generating σS_i follows the general formula given in Eq. 2. σS_i were then used to define fitting and interpolation errors within exponential regressions.

For D_r values, systematic errors accommodate uncertainty in radionuclide conversion factors (5%), β attenuation coefficients (5%), a-value (4%; derived from a systematic α source uncertainty of 3.5% and experimental error), matrix density (0.20g.cm^{-3}), vertical thickness of sampled section (specific to sample collection device), saturation moisture content (3%), moisture content attenuation (2%), burial moisture content (25% relative, unless direct evidence exists of the magnitude and period of differing content), and NaI gamma spectrometer calibration (3%). Experimental errors are associated with radionuclide quantification for each sample by NaI and Ge gamma spectrometry.

The propagation of these errors through to age calculation was quantified using the expression,

$$\sigma y\ (\delta y/\delta x) = (\Sigma\ ((\delta y/\delta x_n).\sigma x_n)^2)^{1/2} \qquad \text{Eq. 2}$$

where y is a value equivalent to that function comprising terms x_n and where σy and σx_n are associated uncertainties.

Errors on age estimates are presented as combined systematic and experimental errors and experimental errors alone. The former (combined) error should be considered when comparing luminescence ages herein with independent chronometric controls. The latter assumes systematic errors are common to luminescence age estimates generated by means identical to those detailed herein and enable direct comparison with those estimates.

5. BAYESIAN CHRONOLOGICAL MODELLING

5.1 Description of Bayesian Approach

The Bayesian approach to the interpretation of archaeological chronologies has been described by Buck *et al* (1996). It is based on the principle that although calibrated radiocarbon dates or luminescence ages accurately estimate the calendar dates of the samples themselves, it is the dates of archaeological events associated with those samples that are important. Bayesian techniques can provide realistic estimates of the dates of such events by combining calendar dating evidence, such as scientific dates with relative dating evidence, such as the stratigraphic relationships between samples. These 'posterior density estimates', (which, by convention, are always expressed *in italics*) are not absolute. They are interpretative estimates, which will change as additional data become available or as the existing data are modelled from different perspectives.

The technique used here is a form of Markov Chain Monte Carlo sampling, which has been applied using the program OxCal v4.1 (Bronk Ramsey 1995; 1998; 2001; 2009). An OxCal model is constructed explicitly specifying the known or assumed relative ages of the dated samples. The model structure is typically defined by the site's Harris matrix. The program calculates the probability distributions of the individual calibrated radiocarbon dates (Stuiver and Reimer 1993) and luminescence ages, and then attempts to reconcile these distributions with the relative ages of the samples, by repeatedly sampling each distribution (using the Metropolis-Hastings algorithm) to build up the set of solutions consistent with the model structure.

This process produces a posterior density estimate of each sample's calendar age, which occupies only part of the prior probability distribution. The posterior distribution is then compared to the prior distribution; an index of agreement is calculated that reflects the consistency of the two distributions. If the posterior distribution is situated in a high-probability region of the prior distribution, the index of agreement is high (sometimes 100 or more). If the index of agreement falls below 60 (a threshold value analogous to the 0.05 significance level in a χ^2 test), however, the scientific date is regarded as inconsistent

with the sample's calendar age, if the latter is consistent with the sample's age relative to the other dated samples. Sometimes this merely indicates that the scientific date is a statistical outlier, but a very low index of agreement may indicate either then there is a scientific issue with the date (eg incomplete bleaching) or that the sampled material was residual or intrusive (ie that its calendar age is different to that implied by its stratigraphic position).

An overall index of agreement is calculated from the individual agreement indices, providing a measure of the consistency between the archaeological phasing and the radiocarbon results. Again, this has a threshold value of 60. The program is also able to calculate distributions for the dates of events that have not been dated directly, such as the beginning and end of a continuous phase of activity (which is represented by several scientific dates), and for the durations of phases of activity or hiatuses between such phases.

5.2 Chronological Model for earthwork system so6013/04

Following the construction of earthwork bank (104), two distinct layers of colluvium built up behind it ((107) and (103)). Two radiocarbon measurements (OxA-25372 and SUERC-36801) and a luminescence age (GL11018) are available from (107), and one luminescence age is available from (103)(GL11019). Later than this was a charcoal-rich deposit of bloomery slag, from which came two radiocarbon dates (OxA-25373 and SUERC-36802).

A chronological model which incorporates this stratigraphic sequence (Fig 1), with the scientific dating information is shown in Figure 11. This model has poor overall agreement (Amodel:12; Fig 11; Bronk Ramsey 1995, 429), as GL11019 from context (103) is clearly too old in relation to the dates from context (107) below. This sample has very poor individual agreement (A:3).

A revised model was therefore constructed, which interprets GL11019 as anomalous and excludes it from the analysis. This model is shown in Figure 12. This has good overall agreement (Amodel:100; Fig 12). This model suggests that the earthwork system was laid out in *940–260 cal BC (95% probability; build so6013/04*; Fig 12), probably in *580–385 cal BC (68% probability)*. The iron-working activity is probably most reliably dated by the later of the two fragments of charcoal incorporated within context (116), dating to *cal AD 20–135 (95% probability; OxA-25373*; Fig 12), probably to *cal AD 60–120 (68% probability).*

5.3 Chronological model for earthwork system so6013/26

Two luminescence ages have been produced from the colluvium in Trench 2, with sample FOD03 being earlier than sample FOD04 (Fig 2). In the absence of earthworks in the trench, the relationship between the terracing and the colluvium is inferred. Nonetheless,

the reported luminescence ages are in good agreement with the relative stratigraphic sequence of the samples (Amodel:106; Fig 13) and GL11021 is compatible with finds of abraded Roman pottery from the colluvium. Given the potential for incomplete bleaching in these deposits, however (Table 3), it can only be suggested that the earthwork system is later than the last centuries of the first millennium BC (*GL11020*; Fig 13).

6. CONCLUSIONS

A series of radiocarbon dates and optically stimulated luminescence ages were obtained from colluvium and overlying deposits, which had built up behind a bank related to earthwork system so6013/04. Bayesian chronological modelling of these scientific dates, along with the recorded stratigraphic sequence, suggests that this earthwork system may have been laid out in the mid first millennium cal BC. An overlying deposit containing iron-working debris, probably dates to the late first or early second century cal AD.

Two ages were by optically stimulated luminescence from colluvium that may be related to earthwork system so6013/26. These dates demonstrate that this earthwork system was laid out in, or after, the latter part of the first millennium cal BC.

7. BIBLIOGRAPHY

Adamiec, G, and Aitken, M J, 1998 Dose-rate conversion factors: new data, *Ancient TL*, **16**, 37–50

Aitken, M J, 1998 *An introduction to optical dating: the dating of Quaternary sediments by the use of photon-stimulated luminescence*, Oxford (Oxford Univ Press)

Agersnap-Larsen, N, Bulur, E, Bøtter-Jensen, L, and McKeever, S W S, 2000 Use of the LM-OSL technique for the detection of partial bleaching in quartz, *Radiation Measurements*, **32**, 419–25

Bailey, R M, Singarayer, J S, Ward, S, and Stokes, S, 2003 Identification of partial resetting using D_e as a function of illumination time, *Radiation Measurements*, **37**, 511–18

Bateman, M D, Frederick, C D, Jaiswal, M K, Singhvi, A K, 2003 Investigations into the potential effects of pedoturbation on luminescence dating, *Quaternary Science Reviews*, **22**, 1169–76

Berger, G W, 2003 Luminescence chronology of late Pleistocene loess-paleosol and tephra sequences near Fairbanks, Alaska, *Quaternary Research*, **60**, 70–83

Bøtter-Jensen, L, Mejdahl, V, and Murray, A S, 1999 New light on OSL, *Quaternary Science Reviews*, **18**, 303–10

Bøtter-Jensen, L, McKeever, S W S, and Wintle, A G, 2003 *Optically Stimulated Luminescence Dosimetry*, Amsterdam (Elsevier)

Brock, F, Higham, T, Ditchfield, P, and Bronk Ramsey, C, 2010 Current pretreatment methods for AMS radiocarbon dating at the Oxford Radiocarbon Accelerator Unit (ORAU), *Radiocarbon*, **52**, 103–12

Bronk Ramsey, C, 1995 Radiocarbon calibration and analysis of stratigraphy, *Radiocarbon*, **36**, 425–30

Bronk Ramsey, C, 1998 Probability and dating, *Radiocarbon*, **40**, 461–74

Bronk Ramsey, C, 2001 Development of the radiocarbon calibration program, *Radiocarbon*, **43**, 355–63

Bronk Ramsey, C, 2009 Bayesian analysis of radiocarbon dates, *Radiocarbon,* **51**, 337–60

Bronk Ramsey, C, Higham, T, and Leach, P, 2004 Towards high precision AMS: progress and limitations, *Radiocarbon*, **46**, 17–24

Buck, C E, Cavanagh, W G, and Litton, C D, 1996 *Bayesian Approach to Interpreting Archaeological Data*, Chichester

Dee, M, and Bronk Ramsey, C, 2000 Refinement of the graphite target production at ORAU, *Nuclear Instruments and Methods in Physics Research, B*, **172**, 449–53

Duller, G A T, 2003 Distinguishing quartz and feldspar in single grain luminescence measurements, *Radiation Measurements*, **37**, 161–5

Galbraith, R F, 1990 The radial plot: graphical assessment of spread in ages, *Nuclear Tracks and Radiation Measurements*, **17**, 207–14

Galbraith, R F, Roberts, R G, Laslett, G M, Yoshida, H, and Olley, J M, 1999 Optical dating of single and multiple grains of quartz from Jinmium rock shelter (northern Australia): Part I, Experimental design and statistical models, *Archaeometry*, **41**, 339–64

Hubbell, J H, 1982 Photon mass attenuation and energy-absorption coefficients from 1keV to 20MeV, *International Journal of Applied Radioisotopes*, **33**, 1269–90

Huntley, D J, Godfrey-Smith, D I, and Thewalt, M L W, 1985 Optical dating of sediments, *Nature*, **313**, 105–7

Hütt, G, Jaek, I, and Tchonka, J, 1988 Optical dating: K-feldspars optical response stimulation spectra, *Quaternary Science Reviews*, **7**, 381–6

Markey, B G, Bøtter-Jensen, L, and Duller, G A T, 1997 A new flexible system for measuring thermally and optically stimulated luminescence, *Radiation Measurements*, **27**, 83–9

Mejdahl, V, 1979 Thermoluminescence dating: beta-dose attenuation in quartz grains, *Archaeometry*, **21**, 61–72

Murray, A S, and Olley, J M, 2002 Precision and accuracy in the Optically Stimulated Luminescence dating of sedimentary quartz: a status review, *Geochronometria*, **21**, 1–16

Murray, A S, and Wintle, A G, 2000 Luminescence dating of quartz using an improved single-aliquot regenerative-dose protocol, *Radiation Measurements*, **32**, 57–73

Murray, A S, and Wintle, A G, 2003 The single aliquot regenerative dose protocol: potential for improvements in reliability, *Radiation Measurements*, **37**, 377–81

Murray, A S, Olley, J M, and Caitcheon, G G, 1995 Measurement of equivalent doses in quartz from contemporary water-lain sediments using optically stimulated luminescence, *Quaternary Science Reviews*, 14, 365–71

Olley, J M, Murray, A S, and Roberts, R G, 1996 The effects of disequilibria in the Uranium and Thorium decay chains on burial dose rates in fluvial sediments, *Quaternary Science Reviews*, **15**, 751–60

Olley, J M, Caitcheon, G G, and Murray, A S, 1998 The distribution of apparent dose as determined by optically stimulated luminescence in small aliquots of fluvial quartz: implications for dating young sediments, *Quaternary Science Reviews*, **17**, 1033–40

Olley, J M, Caitcheon, G G, and Roberts, R G, 1999 The origin of dose distributions in fluvial sediments, and the prospect of dating single grains from fluvial deposits using - optically stimulated luminescence, *Radiation Measurements*, **30,** 207–17

Olley, J M, Pietsch, T, and Roberts, R G, 2004 Optical dating of Holocene sediments from a variety of geomorphic settings using single grains of quartz, *Geomorphology*, **60**, 337–58

Pawley, S M, Toms, P S, Armitage, S J, Rose, J, 2010 Quartz luminescence dating of Anglian Stage fluvial sediments: Comparison of SAR age estimates to the terrace chronology of the Middle Thames valley, UK, *Quaternary Geochronology*, **5**, 569–82

Prescott, J R, and Hutton, J T, 1994 Cosmic ray contributions to dose rates for luminescence and ESR dating: large depths and long-term time variations, *Radiation Measurements*, **23**, 497–500

Reimer, P, Baillie, M, Bard, E, Bayliss, A, Beck, J, Blackwell, P, Bronk Ramsey , C, Buck, C, Burr, G, Edwards, R, Friedrich, M, Grootes, P, Guilderson, T, Hajdas, I, Heaton, T, Hogg, A, Hughen, K, Kaiser, K, Kromer, B, McCormac, F, Manning, S, Reimer, R, Richards, D, Southon, J, Talamo, S, Turney, C, van der Plicht, J, and Weyhenmeyer, C, 2009 INTCAL09 and MARINE09 radiocarbon age calibration curves, 0–50,000 years Cal BP, *Radiocarbon*, **51**, 1111–50

Scott, E, Cook, G, and Naysmith, P, 2010 The fifth international radiocarbon intercomparison (VIRI): an assessment of laboratory performance in stage 3, *Radiocarbon* **53**, 859–65

Singhvi, A K, Bluszcz, A, Bateman, M D, Someshwar Rao, M, 2001 Luminescence dating of loess-palaeosol sequences and coversands: methodological aspects and palaeoclimatic implications, *Earth Science Reviews*, **54**, 193–211

Slota Jr, P J, Jull, A J T, Linick, T W, and Toolin, L J, 1987 Preparation of small samples for radiocarbon accelerator targets by catalytic reduction of CO, *Radiocarbon* **29**, 303–6

Smith, B W, Rhodes, E J, Stokes, S, Spooner, N A, 1990 The optical dating of sediments using quartz, *Radiation Protection Dosimetry*, **34**, 75–8

Spooner, N A, 1993 The validity of optical dating based on feldspar, Unpubl DPhil thesis, Oxford Univ

Stenhouse, M J, and Baxter, M S, 1983 ^{14}C dating reproducibility: evidence from routine dating of archaeological samples, *PACT* **8**, 147–61

Stuiver, M, and Kra, R S, 1986 Editorial comment, *Radiocarbon*, **28**(2B), ii

Stuiver, M, and Polach, H A, 1977 Reporting of ^{14}C data, *Radiocarbon*, **19**, 355–63

Stuiver, M, and Reimer, P J, 1986 A computer program for radiocarbon age calculation, *Radiocarbon*, **28**, 1022–30

Stuiver, M, and Reimer, P J, 1993 Extended ^{14}C data base and revised CALIB 3.0 ^{14}C age calibration program, *Radiocarbon*, **35**, 215-30

Templer, R H, 1985 The removal of anomalous fading in zircons, *Nuclear Tracks and Radiation Measurements*, **10**, 531–7

Vandeputte, K, Moens, L, and Dams, R, 1996 Improved sealed-tube combustion of organic samples to CO_2 for stable isotope analysis, radiocarbon dating and percent carbon determinations, *Analytical Letters* **29**, 2761–73

Wallinga, J, 2002 Optically stimulated luminescence dating of fluvial deposits: a review, *Boreas*, **31**, 303–22

Ward, G K, and Wilson, S R, 1978 Procedures for comparing and combining radiocarbon age determinations: a critique, *Archaeometry,* **20**, 19–31

Wintle, A G, 1973 Anomalous fading of thermoluminescence in mineral samples, *Nature*, **245**, 143–4

Xu, S, Anderson, R, Bryant, C, Cook, G T, Dougans, A, Freeman, S, Naysmith, P, Schnabel, C, and Scott, E M, 2004 Capabilities of the new SUERC 5MV AMS facility for ^{14}C dating, *Radiocarbon*, **46**, 59–64

Zimmerman, D W, 1971 Thermoluminescent dating using fine grains from pottery, *Archaeometry*, **13**, 29–52

Table 1: Results of radiocarbon and stable isotope analyses from Cannop Trench 1

Laboratory number	Sample	Radiocarbon age (BP)	δ13C (‰)	Calibrated date (95% confidence)
SUERC-36801	37920/107a. Corylus avellana truck/branchwood charcoal.	2330±30	–24.0	410–380 cal BC
OxA-25372	37920/107b <6>. Corylus avellana truck/branchwood charcoal.	2268±26	–24.01	400–210 cal BC
SUERC-36802	37920/116a. Quercus sp. roundwood charcoal of *c*10 years growth.	1975±30	–25.2	50 cal BC–cal AD 90
OxA-25373	37920/116b <4>. Alnus sp. roundwood charcoal.	1911±26	–23.64	cal AD 20–140

Table 2a: D_r data of submitted samples. Site located at c 52°N, 3°W, 120m. Blue indicates samples with accepted age estimates, red, age estimates with caveats (see Table 3)

Field Code	Lab Code	Overburden (m)	Moisture content (%)	γ D_r ($Gy.ka^{-1}$)	β D_r ($Gy.ka^{-1}$)	Cosmic D_r ($Gy.ka^{-1}$)	Total D_r ($Gy.ka^{-1}$)
FOD01	GL11018	0.77	9 ± 2	0.89 ± 0.08	1.38 ± 0.12	0.19 ± 0.02	2.46 ± 0.14
FOD02	GL11019	0.44	12 ± 3	0.81 ± 0.08	1.21 ± 0.11	0.20 ± 0.02	2.22 ± 0.14
FOD03	GL11020	0.50	15 ± 4	0.77 ± 0.08	1.20 ± 0.12	0.20 ± 0.02	2.16 ± 0.15
FOD04	GL11021	0.30	15 ± 4	0.77 ± 0.08	1.21 ± 0.12	0.20 ± 0.03	2.19 ± 0.16

Table 2b: D_e and Age data of submitted samples. Age estimates processed from 125–180µm quartz fraction for samples GL11018 and GL11019, 180–250µm quartz for GL11020 and GL11021. Uncertainties in age are quoted at 1σ confidence, are based on analytical errors and reflect combined systematic and experimental variability and (in parenthesis) experimental variability alone (see §4.6). Blue indicates samples with accepted age estimates, red, age estimates with caveats (see Table 3)

Field Code	Lab Code	Preheat (°C for 10s)	Low Dose Repeat Ratio	High Dose Repeat Ratio	Post-IR OSL Ratio	D_e (Gy)	Age (ka before 2011)	Date
FOD01	GL11018	260	0.98 ± 0.02	0.98 ± 0.01	0.99 ± 0.01	5.0 ± 0.2	2.0 ± 0.1 (0.1)	133 AD-154 BC
FOD02	GL11019	270	1.00 ± 0.02	0.98 ± 0.03	0.99 ± 0.02	6.3 ± 0.2	2.8 ± 0.2 (0.2)	595 BC-1010 BC
FOD03	GL11020	240	0.98 ± 0.02	0.98 ± 0.02	1.01 ± 0.02	4.6 ± 0.2	2.1 ± 0.2 (0.1)	56 AD-304 BC
FOD04	GL11021	240	1.00 ± 0.03	0.98 ± 0.02	0.99 ± 0.04	4.0 ± 0.2	1.8 ± 0.2 (0.1)	345 AD-1AD

Table 3: Analytical validity of sample suite age estimates and caveats for consideration

Generic considerations	Field Code	Lab Code	Sample specific considerations
None	FOD01	GL11018	None
	FOD02	GL11019	None
	FOD03	GL11020	Limited datable mass Possible partial bleaching (see §4.3.2 and Fig 8c)
	FOD04	GL11021	Possible partial bleaching (see §4.3.2 and Fig 8d)

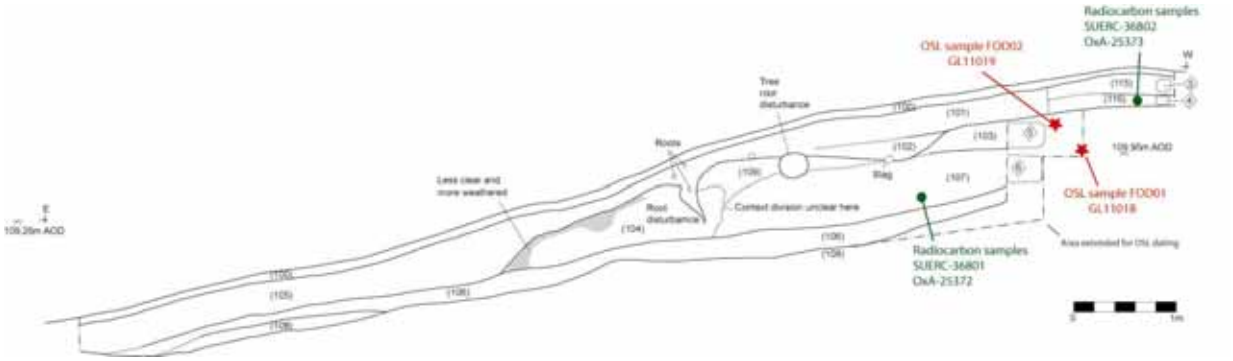

Figure 1: Location of samples for scientific dating from earthwork system so6013/04 (Cannop Trench 1)

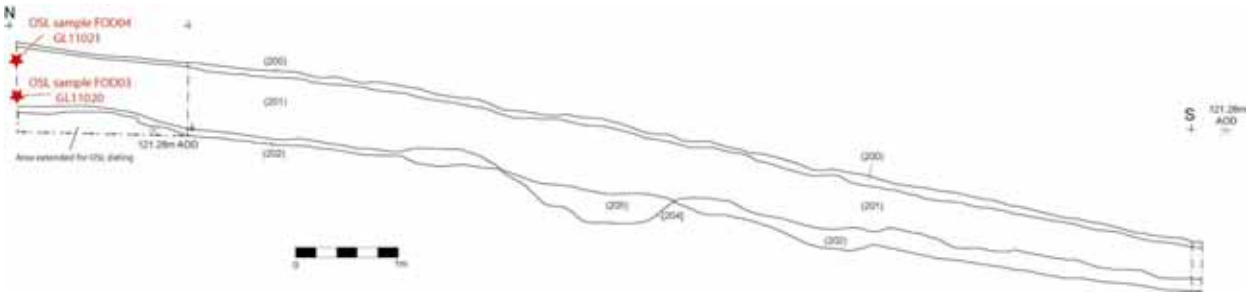

Figure 2: Location of samples for scientific dating from earthwork system so6013/26 (Cannop Trench 2)

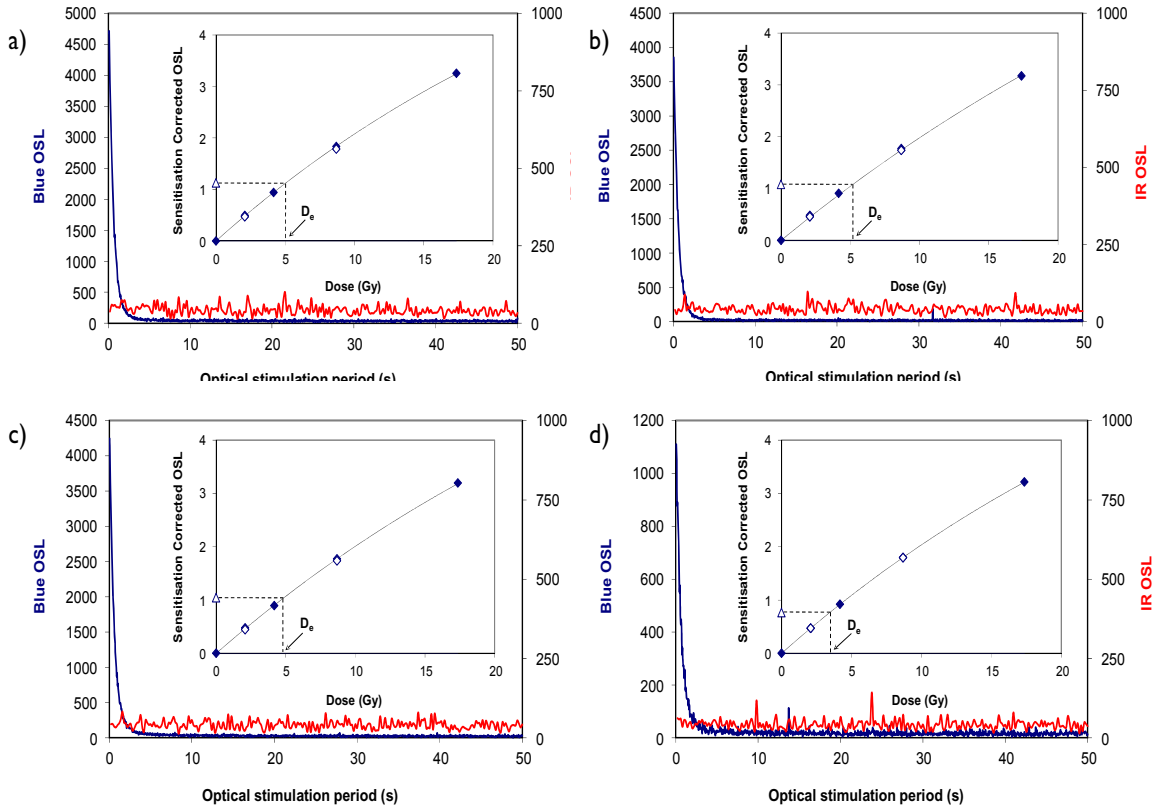

Figure 3: Signal Calibration for samples a) GL11018, b) GL11019, c) GL11020 and d) GL11021. Natural blue and laboratory-induced infrared (IR) OSL signals. Detectable IR signal decays are diagnostic of feldspar contamination. Inset, the natural blue OSL signal (open triangle) of each aliquot is calibrated against known laboratory doses to yield equivalent dose (D_e) values. Repeats of low and high doses (open diamonds) illustrate the success of sensitivity correction

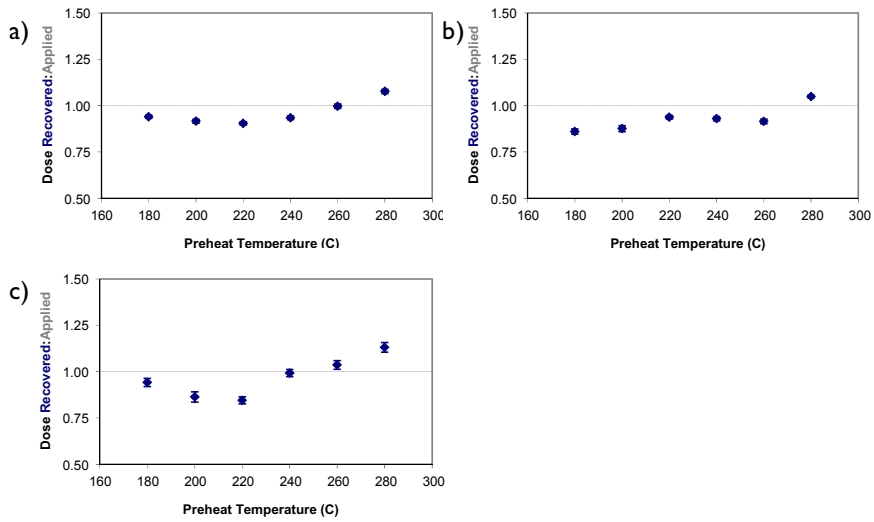

Figure 4: Dose Recovery test for samples a) GL11018, b) GL11019 and c) GL11021 (insufficient datable material for GL11020). The acquisition of D_e values is necessarily predicated upon thermal treatment of aliquots succeeding environmental and laboratory irradiation. The Dose Recovery test quantifies the combined effects of thermal transfer and sensitisation on the natural signal using a precise lab dose to simulate natural dose. Based on this an appropriate thermal treatment is selected to generate the final D_e value

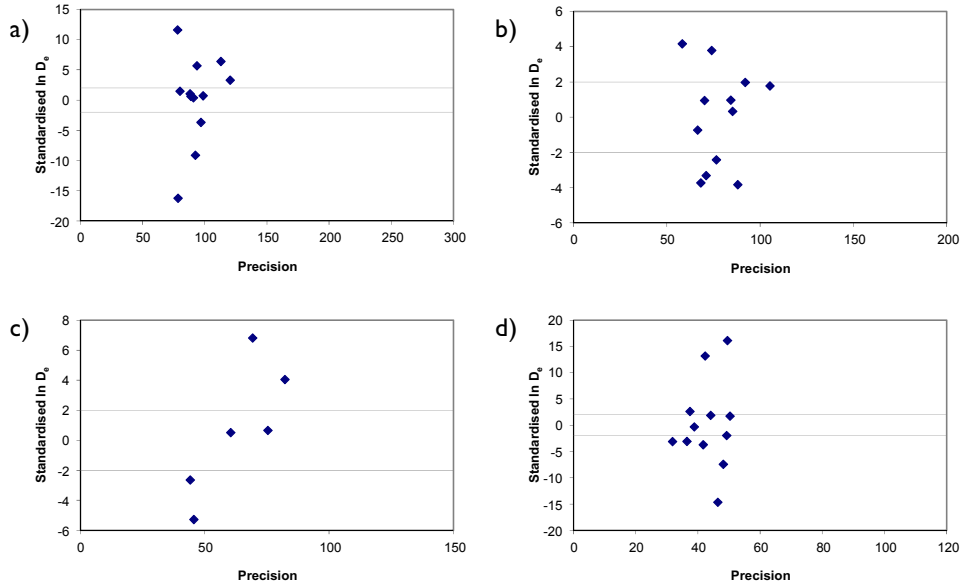

Figure 5: Inter-aliquot D_e distribution for samples a) GL11018, b) GL11019, c) GL11020 and d) GL11021. Provides a measure of inter-aliquot statistical concordance in D_e values derived from natural irradiation. Discordant data (those points lying beyond ±2 standardised ln D_e) reflects heterogeneous dose absorption and/or inaccuracies in calibration

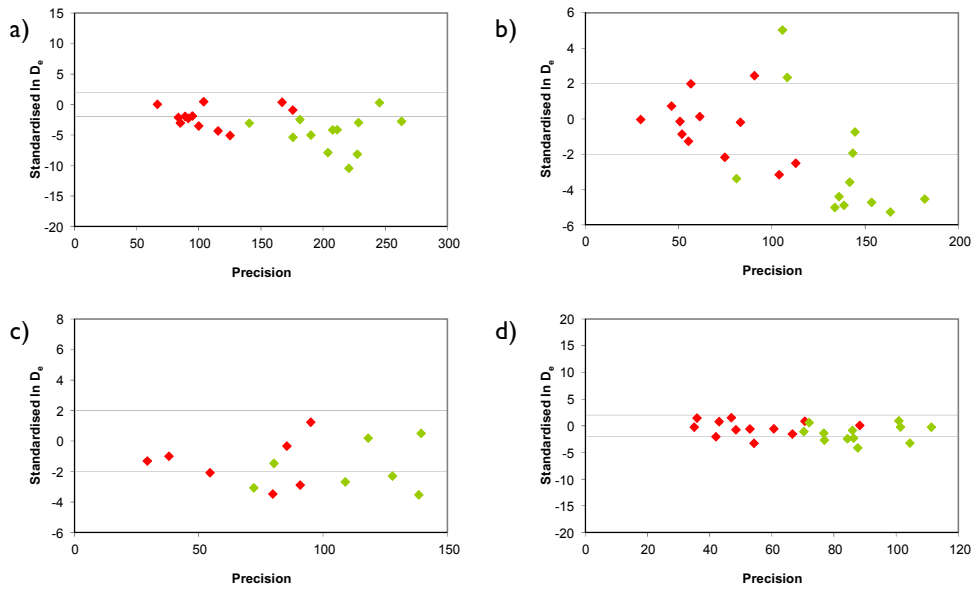

*Figure 6: Low and High Repeat Regenerative-dose Ratio for samples a) GL11018, b) GL11019, c) GL11020 and d) GL11021. Measures the statistical concordance of signals from repeated **low** and **high** regenerative-doses. Discordant data (those points lying beyond ±2 standardised ln D_e) indicate inaccurate sensitivity correction*

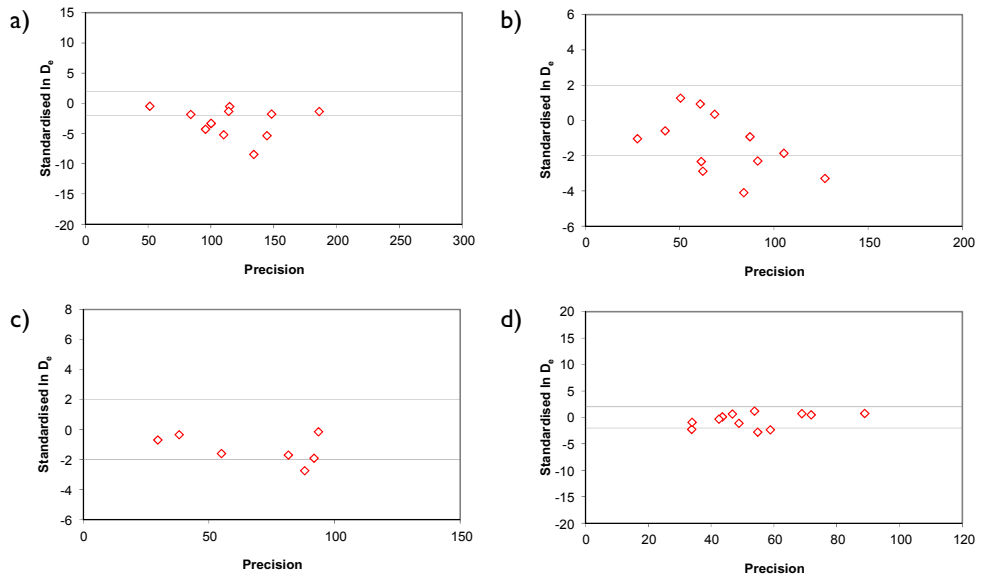

Figure 7: OSL to Post-IR OSL Ratio for samples a) GL11018, b) GL11019, c) GL11020 and d) GL11021. Measures the statistical concordance of OSL and post-IR OSL responses to the same regenerative-dose. Discordant, underestimating data (those points lying below -2 standardised ln D_e) and the presence of an IRSL signal (Fig 3) would highlight the presence of significant feldspar contamination

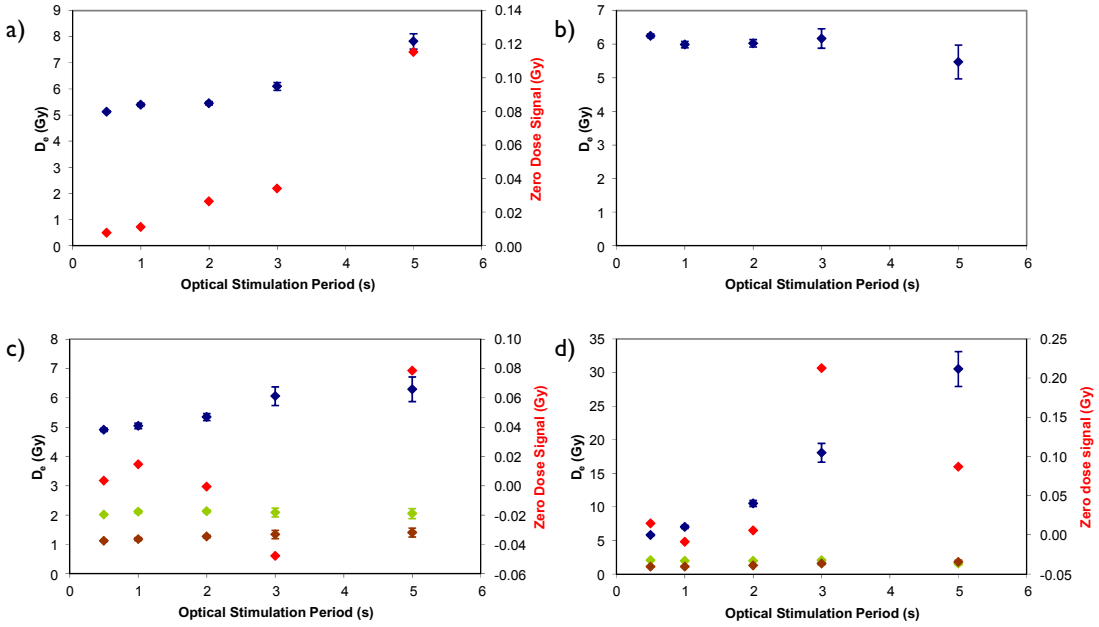

Figure 8: Signal Analysis for samples a) GL11018, b) GL11019, c) GL11020 and d) GL11021. Statistically significant increase in ***natural*** *D_e value with signal stimulation period is indicative of a partially-bleached signal, provided a significant increase in D_e results from* ***simulated partial bleaching*** *followed by insignificant adjustment in D_e for simulated* ***zero*** *and* ***full bleach*** *conditions. Ages from such samples are considered maximum estimates. In the absence of a significant rise in D_e with stimulation time, simulated partial bleaching and zero/full bleach tests are not assessed*

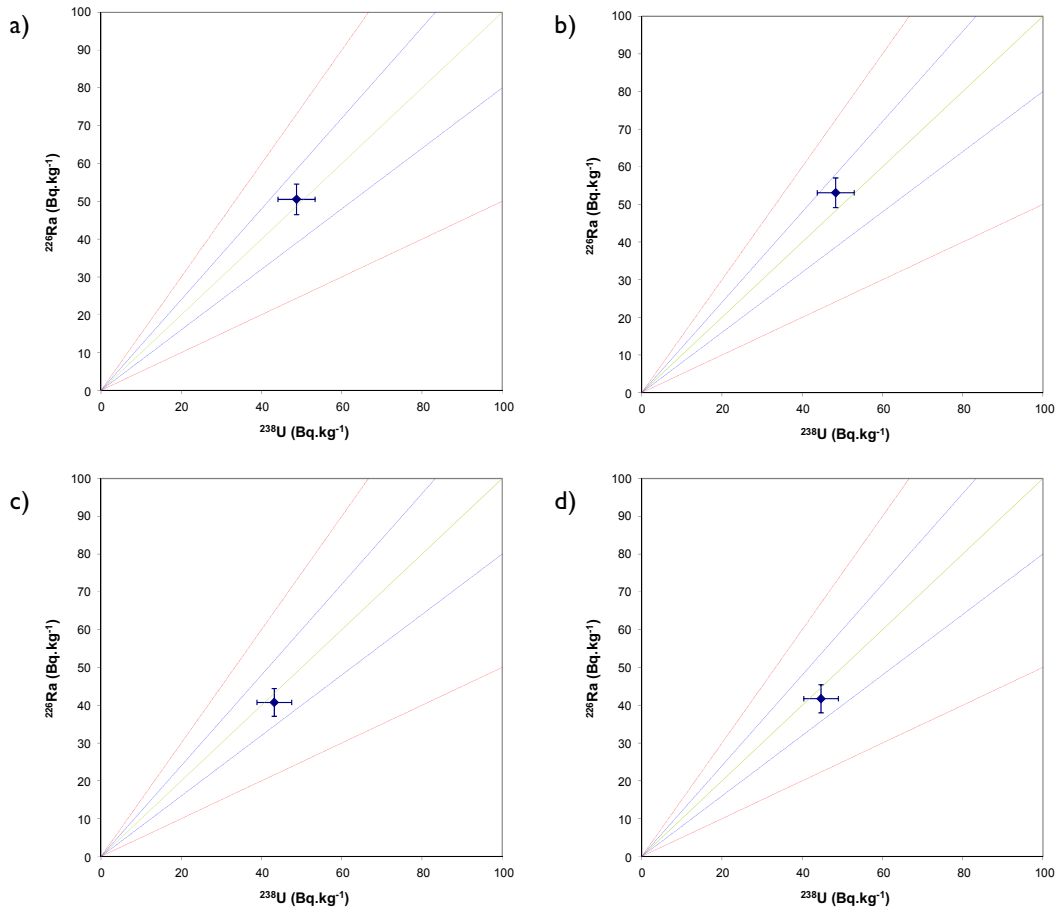

*Figure 9: U activity for samples a) GL11018, b) GL11019, c) GL11020 and d) GL11021. Statistical concordance (equilibrium) in the activities of the daughter radioisotope ^{226}Ra with its parent ^{238}U may signify the temporal stability of D_r emissions from these chains. Significant differences (disequilibrium; **>50%**) in activity indicate addition or removal of isotopes creating a time-dependent shift in D_r values and increased uncertainty in the accuracy of age estimates. A **20%** disequilibrium marker is also shown*

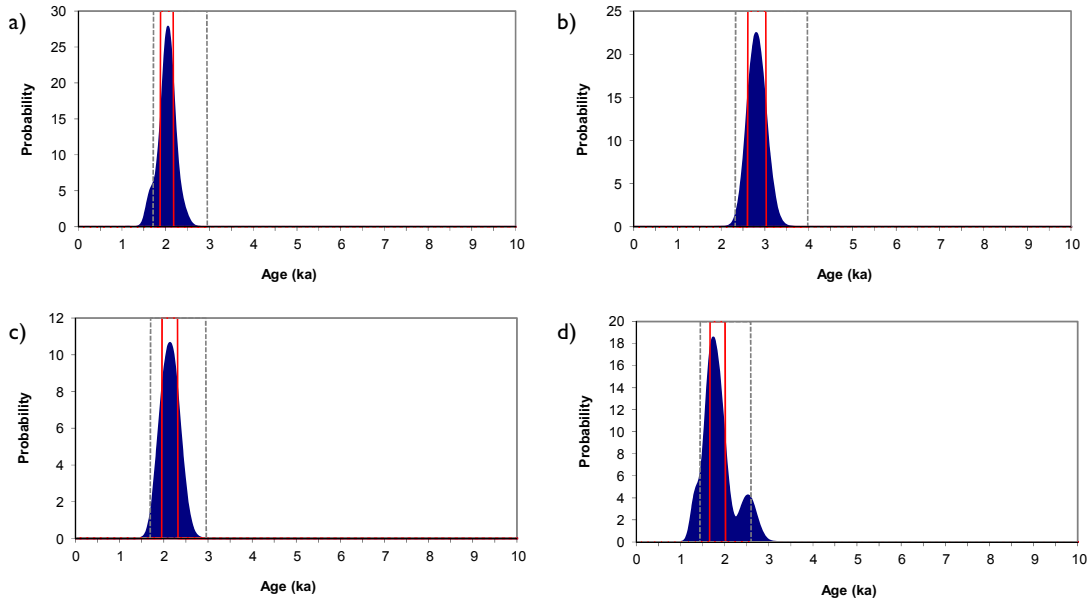

Figure 10: Age Range for samples a) GL11018, b) GL11019, c) GL11020 and d) GL11021. The ***mean age range*** *provides an estimate of sediment burial period based on mean D_e and D_r values with associated analytical uncertainties. The* ***probability distribution*** *offers an illustration of inter-aliquot variability in age. The* ***maximum influence*** *of temporal variations in D_r forced by minima-maxima variation in moisture content and overburden thickness may prove instructive where there is uncertainty in these parameters, however the combined extremes represented should not be construed as preferred age estimates*

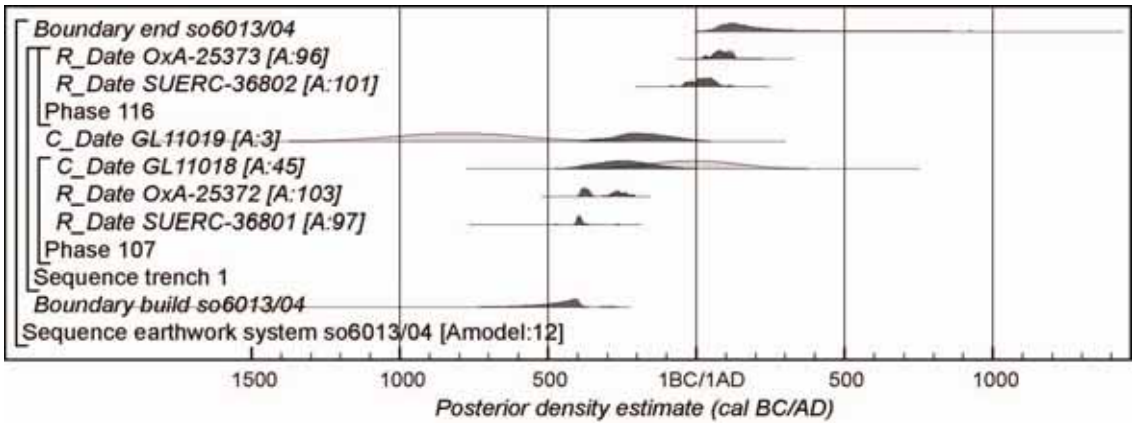

Figure 11: Probability distributions of dates from earthwork system so6013/04, infilling behind the bank is assumed to have been relatively constant and continuous. Each distribution represents the relative probability that an event occurs at a particular time. For each scientific date, two distributions have been plotted: one in outline which is the simple scientific date, and a solid one based on the chronological model used. The other distributions correspond to aspects of the model. For example, the distribution 'build so6013/04 is the posterior density estimate for the time when the earthwork was constructed. The large square brackets down the left-hand side of the diagram and the OxCal keywords define the overall model exactly

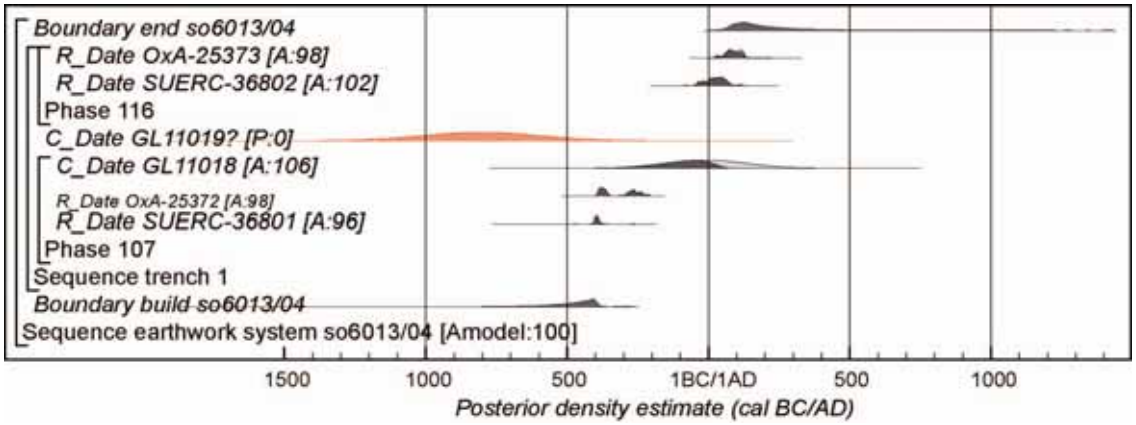

Figure 12: Probability distributions of dates from earthwork system so6013/04, infilling behind the bank is assumed to have been relatively constant and continuous (with GL11019 excluded). The format is identical to that of Figure 11. The large square brackets down the left-hand side of the diagram and the OxCal keywords define the overall model exactly

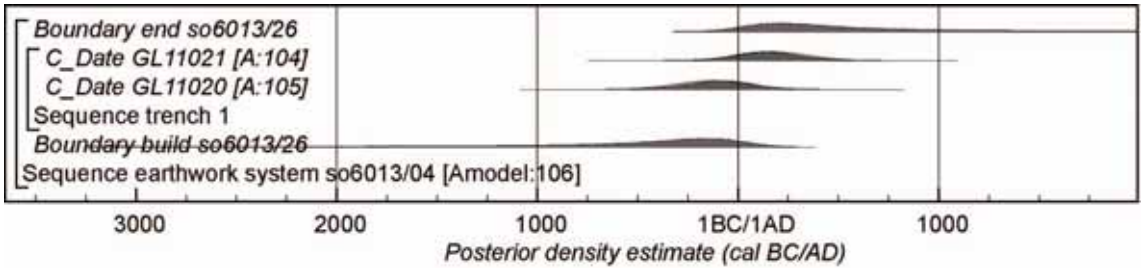

Figure 13: Probability distributions of dates from earthwork system so6013/26. The format is identical to that of Figure 11. The large square brackets down the left-hand side of the diagram and the OxCal keywords define the overall model exactly

ENGLISH HERITAGE RESEARCH AND THE HISTORIC ENVIRONMENT

English Heritage undertakes and commissions research into the historic environment, and the issues that affect its condition and survival, in order to provide the understanding necessary for informed policy and decision making, for the protection and sustainable management of the resource, and to promote the widest access, appreciation and enjoyment of our heritage. Much of this work is conceived and implemented in the context of the National Heritage Protection Plan. For more information on the NHPP please go to http://www.english-heritage.org.uk/professional/protection/national-heritage-protection-plan/.

The Heritage Protection Department provides English Heritage with this capacity in the fields of building history, archaeology, archaeological science, imaging and visualisation, landscape history, and remote sensing. It brings together four teams with complementary investigative, analytical and technical skills to provide integrated applied research expertise across the range of the historic environment. These are:

* Intervention and Analysis (including Archaeology Projects, Archives, Environmental Studies, Archaeological Conservation and Technology, and Scientific Dating)
* Assessment (including Archaeological and Architectural Investigation, the Blue Plaques Team and the Survey of London)
* Imaging and Visualisation (including Technical Survey, Graphics and Photography)
* Remote Sensing (including Mapping, Photogrammetry and Geophysics)

The Heritage Protection Department undertakes a wide range of investigative and analytical projects, and provides quality assurance and management support for externally-commissioned research. We aim for innovative work of the highest quality which will set agendas and standards for the historic environment sector. In support of this, and to build capacity and promote best practice in the sector, we also publish guidance and provide advice and training. We support community engagement and build this in to our projects and programmes wherever possible.

We make the results of our work available through the Research Report Series, and through journal publications and monographs. Our newsletter *Research News*, which appears twice a year, aims to keep our partners within and outside English Heritage up-to-date with our projects and activities.

A full list of Research Reports, with abstracts and information on how to obtain copies, may be found on www.english-heritage.org.uk/researchreports

For further information visit www.english-heritage.org.uk

ENGLISH HERITAGE

ISSN 2046-9799 (Print)
ISSN 2046-9802 (Online)